6 EPR Signals in Methanogens

6.1 Hydrogenothropic Pathway

Fig. 1 shows the CO_2-reducing pathway of methanogenesis, which uses H_2 and CO_2 as substrates. The reduction of CO_2 to CH_4 proceeds via coenzyme-bound C_1-intermediates, methanofuran (MFR), tetrahydromethanopterin (H_4MPT), and coenzyme M (2-mercaptoethanesulfonate, HS-CoM). In the first step CO_2 is reduced to the level of formate: formylmethanofuran. From formylmethanofuran the formyl group is transferred to tetrahydromethanopterin, which serves as the carrier of the C_1 unit during its reduction to methylene- and methyltetrahydromethanopterin. The methyl group is than transferred for the fourth and last reduction step in the pathway to a structurally simple substrate, coenzyme M. Methyl-coenzyme M (CH_3-S-CoM) is reduced with coenzyme B (HS-CoB) to methane and CoM-S-S-CoB. For the reduction steps electrons from the oxidation of H_2 are used. This input is either directly or via coenzyme $F_{420.}$ Hence the most methanogenic bacteria contain two distinct hydrogenases to oxidize H_2: a coenzyme F_{420}-reducing hydrogenase, and a coenzyme F_{420}-non-reducing enzyme. Five enzymes of this pathway are metalloenzymes and will be discussed in the next section.

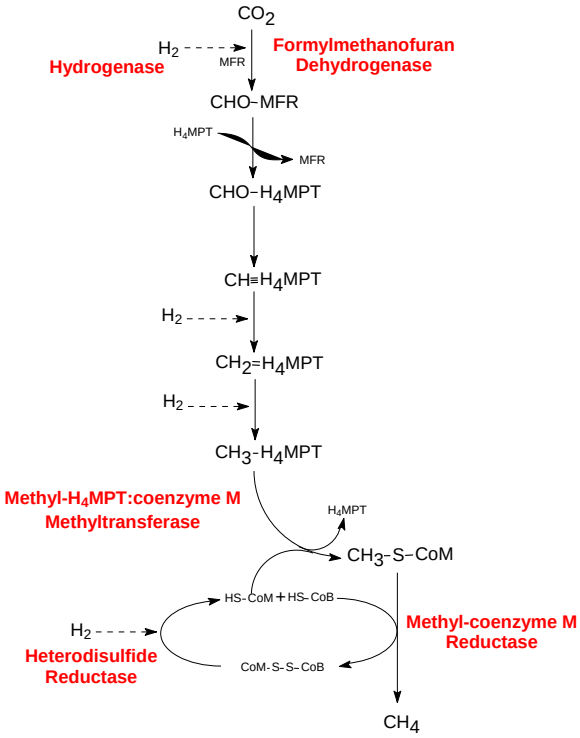

Fig. 1: Metabolic pathway of methanogenesis from CO_2 in *Methanothermobacter marburgensis*. CHO-MFR, N-formylmethanofuran; CHO-H_4MPT, N^5-formyltetrahydromethanopterin; $CH{\equiv}H_4MPT^+$, N^5,N^{10}-methenyltetrahydromethanopterin; $CH_2{=}H_4MPT$, N^5,N^{10}-methylenetetrahydromethanopterin; CH_3-H_4MPT^+, N^5-methyltetrahydromethanopterin; CH_3-S-CoM, methyl-coenzyme M.

6.2 Formylmethanofuran Dehydrogenase

The enzyme (FDH) catalyzes the reversible reduction of CO_2 plus methanofuran (MFR) to *N*-formylmethanofuran (CHO-MFR). FDH contains molybdenum, a molybdopterin dinucleotide, and iron-sulfur clusters.

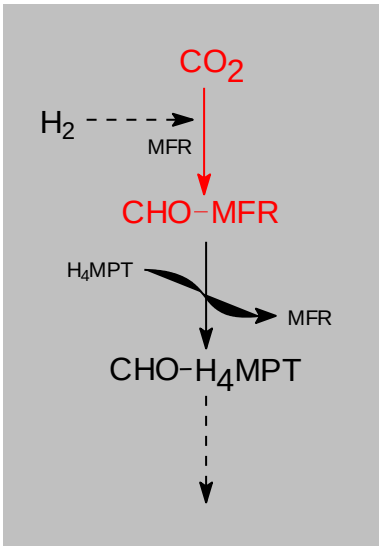

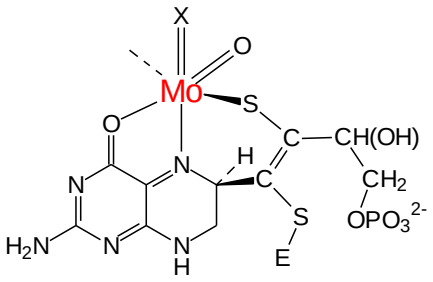

E = H, CH_3 or protein

Fig. 2: Structure of the molybdopterin cofactor

Methanobacterium wolfei contains two active FDH enzymes I and II. FDH I predominated in cells growing in the presence of molybdate and FDH II in cells grown in the presence of tungstate. *M. wolfei* differs from other methanogens in that it can use tungstate as well as molybdate for growth.

The EPR spectrum of active FDH I is depicted in Fig. 3 (trace A). The spectrum of a preparation, which has lost most of its activity due to the loss of Mo is shown in Fig.4 (trace B). This signal is probably due to a [2Fe-2S] cluster. (At lower temperature, 15 K, additional signals could be detected due to [4Fe-4S] clusters.) Fig.4 (trace C) is the difference spectrum of traces A and B, showing the Mo spectrum. Fig. 4 (trace D) shows the spectrum of FDH I purified from cells grown in the presence of ^{97}Mo-molybdate, which has a nuclear spin of I = 5/2.

The EPR spectrum C is composed of two overlapping rhombic signals with only slightly different g values (signal I: g_{xyz} = 2.003, 1.989, 1.955; Signal II: g_{xyz} = 2.00, 19.84, 1.941). It has the characteristics of EPR signals due to Mo^{5+} (d^1). This is particularly demonstrated by the spectrum of the ^{97}Mo-containing enzyme (Fig. 4, trace D). The two overlapping signals are now split.

When *M. wolfei* cells are grown on tungstate, FDH II is expressed. In addition it was found that FDH I was still expressed, but contained W instead of Mo. Fig. 4 (trace A) shows the spectrum of the tungsten-substituted molybdenum FDH I; W^{5+} (d^1) with g_{xyz} = 2.0488, 2.0122, 1.9635. Fig. 4 (trace B) shows a simulation of the spectrum. Fig.4 (Trace B) is a summation of a calculated rhombic S = 1/2 signal without a nuclear hyperfine interaction and the same rhombic signal interacting with a nuclear spin of I = 1/2. The relative intensity of both spectra in the final simulation, 85.6 to 14.4 respectively, was based on the natural abundance of the tungsten isotopes: I = 0: ^{180}W, 0.14%; ^{182}W, 26.4%; ^{184}W, 28.4% and I = 1/2: ^{183}W, 14.4%.

Note that the tungsten EPR signal displayed two g values above 2.0 which is rather unexpected. It has been shown, however, that this is possible for a tungsten(V) complex with a low energy charge transfer exited state.

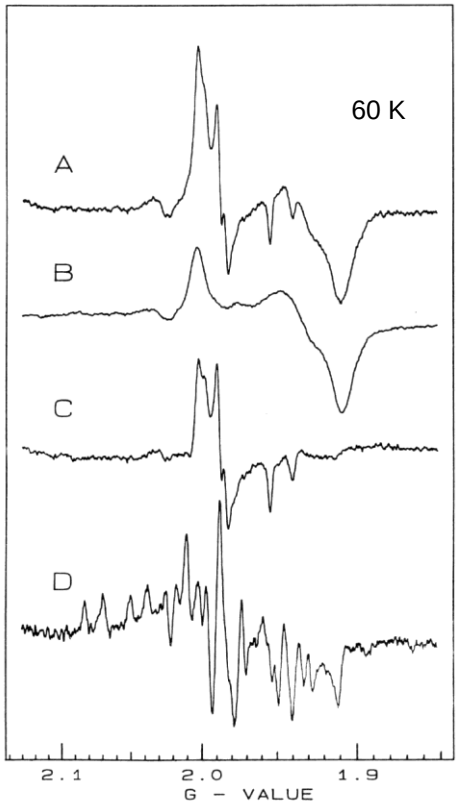

Fig.3: EPR spectra of formylmethanofuran dehydrogenase I from *M. wolfei.*

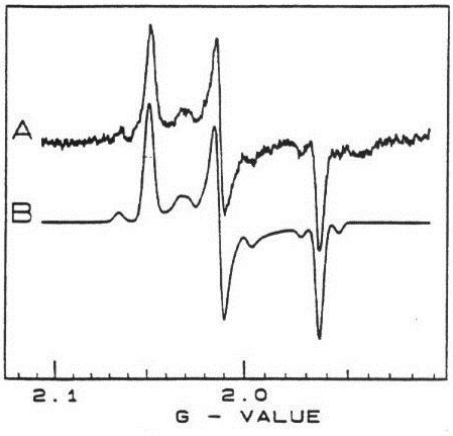

Fig. 4: EPR spectrum of the tungsten-substituted molybdenum formylmethanofuran dehydrogenase I from *M. wolfei*.

References:

Schmitz, R.A., Albracht, S.P.J., Thauer, R.K. (1992) Eur. J. Biochem. 209, 1013-1018.

Schmitz, R.A., Albracht, S.P.J., Thauer, R.K. (1992) FEBS Lett. 309, 78-81.

6.3 Hydrogenase

Hydrogenases catalyze the simple yet important reversible reaction:

$$H_2 \leftrightarrow 2H^+ + 2e^-$$

Through this basic reaction molecular hydrogen is connected to a whole series of metabolic routes. The assimilation of H_2 provides organisms with a supply of reductant which can also be used for energy generation. Alternatively, some organisms dispose of excess reductant in the absence of electron acceptors other than protons by producing H_2.

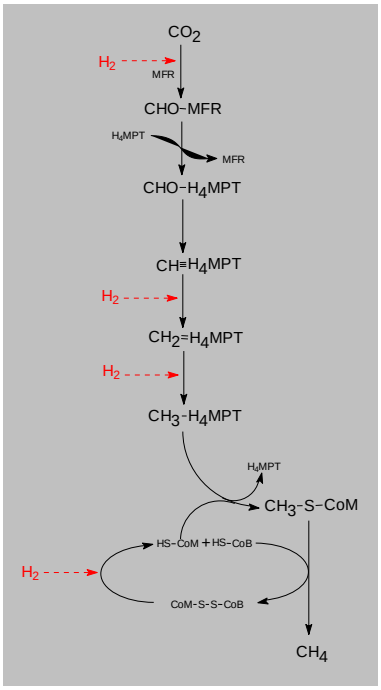

The input of electrons in methanogenesis by oxidation of H_2 is shown in red in the reaction pathway.

Due to the diverse roles of hydrogenases in organisms the enzyme can be either found alone but more often as a part of a larger enzyme complex. The F_{420}-non-reducing hydrogenase from *Methanobacterium marburgensis*, for example, forms a complex with heterodisulfide reductase. The basic unit, however, needed for hydrogenase activity seems to contain two [4Fe-4S] clusters and a dinuclear Ni-Fe center, the place where H_2 binds.

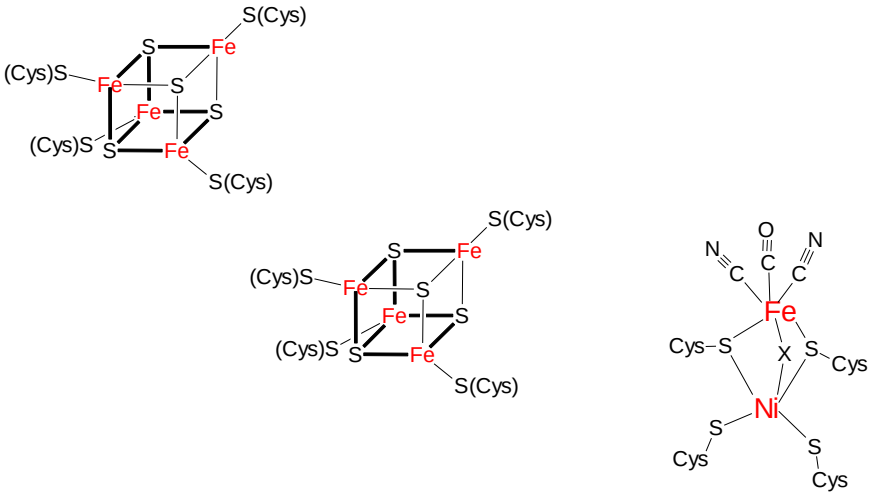

Fig.5: Prosthetic groups found in the minimal hydrogenase unit

It was early realized that hydrogenases might contain nickel, since it was required for the biosynthesis of the enzyme. The actual proof came by showing hyperfine splitting of the EPR signal by using the isotope ^{61}Ni (I = 3/2) (Fig. 6). The discovery that the active site contained iron in addition to the nickel was made when the crystal structure was solved. Since the iron stays in the low-spin 2+ state it is not detectable in EPR spectroscopy.

Fig. 7 shows the different nickel EPR signals found for hydrogenases. In the literature there are two systems for naming the different EPR signals. One is based on redox titrations and involves 3+ (d^7), 2+ (d^8), 1+ (d^9) and 0 (d^{10}) redox states. Since, however, X-ray absorption spectroscopic measurements showed that the electron density on the nickel hardly changes going from 3+ to 1+ the different states are also named A (unready), B (ready), SI (for silent - EPR silent), C (active), and R (for reduced - active and EPR silent). The EPR signal of the C form is light sensitive and the form after illumination is called L. A hydrogen species is expected to bind to the active site at the position of the X in Fig. 5 in the Ni-C state. Upon illumination the bond between this species and the nickel is broken. This was concluded from experiments in D_2O where the illumination reaction is 6 times slower. The origin of the hydrogen species is still not known. Note for example that the nickel EPR signal is not split by the nuclear spin of a H atom (I = 1/2).

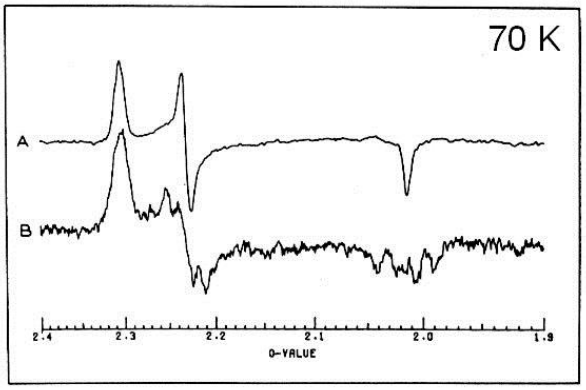

Fig. 6: Comparison of the EPR spectra of hydrogenase from *M. marburgensis* grown on different isotope mixtures: (**A**) growth was performed with natural Ni (natural abundance of ^{61}Ni is 1.19%); (**B**) growth in the presence of ^{61}Ni.

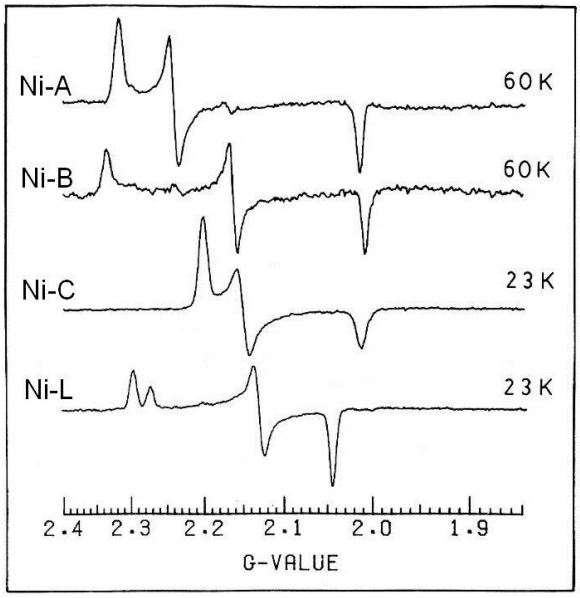

Fig. 7: Different EPR detectable states for hydrogenase from *Chromatium vinosum*.

Reference:

Albracht, S.P.J., Graf, E.-G., Thauer, R.K. (1982) FEBS Lett. 140, 311-313.

6.4 Methyl-H_4MPT:coenzyme M methyltransferase

N^5-Methyltetrahydromethanopterin:coenzyme M methyltransferase (Mtr) from *M. marburgensis* is a membrane-associated enzyme complex, composed of eight different subunits, MtrA-H. MtrA harbors as prosthetic group 5'-hydroxybenzimidazolyl-cobamide:

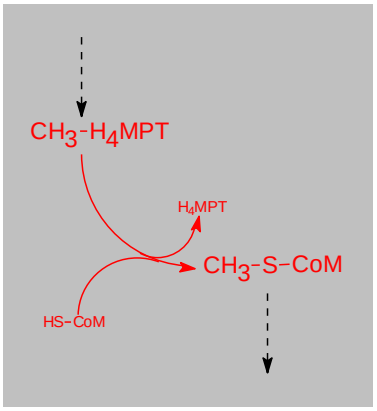

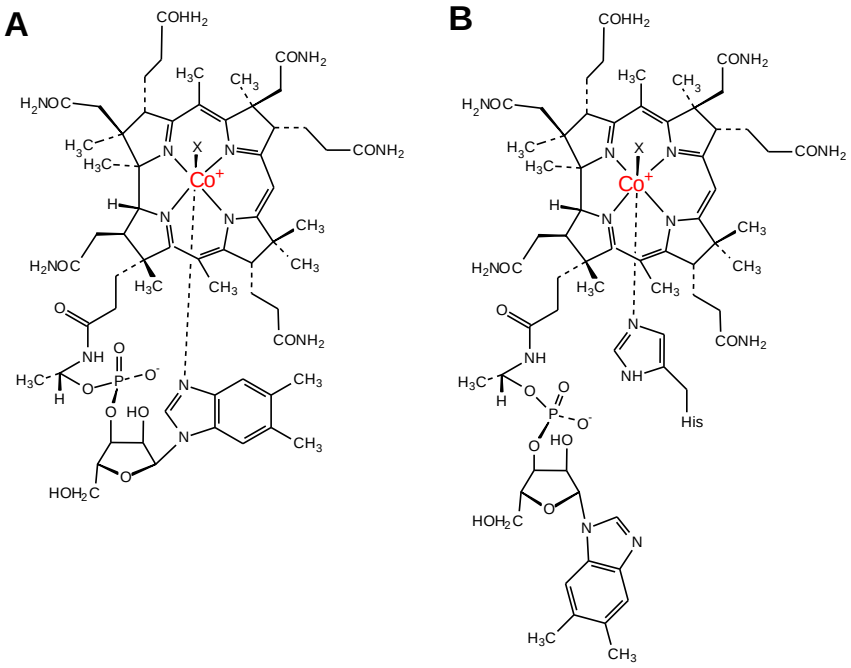

Fig. 8: 5'-hydroxybenzimidazolyl-cobamide in the free, base-on form (**A**) and the protein-bound, base-off form (**B**).

In its super reduced cob(I)amide state this cofactor was shown to accept the methyl group from CH_3-H_4MPT yielding enzyme-bound methyl-cob(III)amide:

$$CH_3\text{-}H_4MPT + E\text{:}CoB(I) \rightarrow H_4MPT + E\text{:}CH_3\text{-}Cob(III)$$

In a second reaction, the methyl group is further transferred to HS-CoM regenerating the enzyme-bound cob(I)amide:

$$E\text{:}CH_3\text{-}CoB(III) + HS\text{-}CoM \rightarrow CH_3\text{-}S\text{-}CoM + E\text{:}CoB(I)$$

Fig. 9 (trace A) shows the EPR spectra of the purified enzyme. Trace B shows a simulation of the spectrum. Characteristics of the Co^{2+} (d^7) spectrum are its g values, g_{xyz} = 2.2591, 2.2530, 2.00659, and the hyperfine splitting of the g_z signal into eight equally spaced lines due to the interaction of the electron with the cobalt nucleus (I = 7/2). The eight lines are further split into triplets, which indicates an interaction of the electron with a ^{14}N-containing axial ligand.

Fig. 10 shows the EPR spectra of the MtrA subunit heterologously overexpressed in *Escherichia coli*. The overexpressed subunit did not contain its corrinoid prosthetic group. Unfolding and refolding in the presence of cobalamin resulted in correctly folded enzyme containing cob(II)alamin. The EPR spectra of the enzyme differentially labeled with ^{14}N (I = 1) and ^{15}N (I = 1/2) revealed that the corrinoid is bound to MtrA in the base-off form and that the Co(II) of the prosthetic group is coordinated by a histidine residue of the apoprotein. Fig. 10, trace B, shows that when the cells were grown on $^{15}NH_4Cl$ the eight lines were split in doublets, proving the axial N ligand came from the enzyme and not from the cofactor itself.

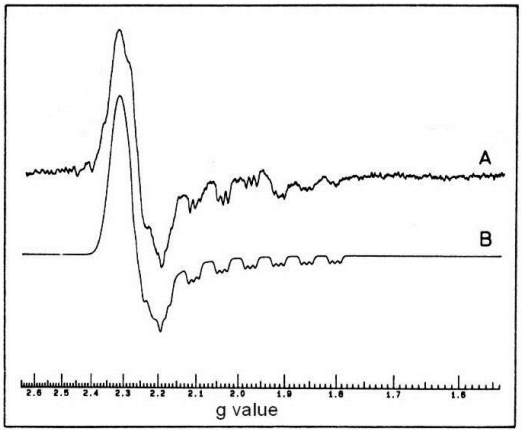

Fig. 9: EPR spectrum of the methyltransferase from *M. marburgensis*. (**A**) Protein as isolated. (**B**) Computer simulation.

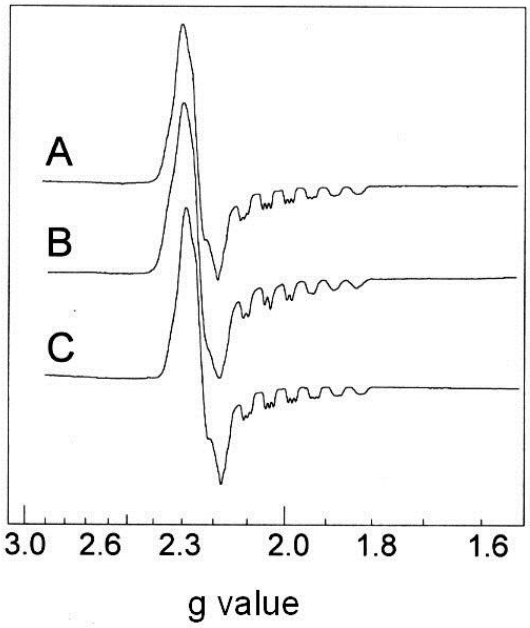

Fig. 10: EPR spectrum of reconstituted MtrA holoprotein in the cob(II)amide oxidation state. (**A**) Holoprotein reconstituted from apoprotein from E. coli cells grown on $^{14}NH_4Cl$ containing medium. (**B**) Holoprotein reconstituted from apoprotein from E. coli cells grown on $^{15}NH_4Cl$ containing medium. (**C**) Holoprotein reconstituted from apoprotein from E. coli cells grown on $^{15}NH_4Cl$ plus [^{14}N]-histidine-containing medium.

References:

Schulz, H., Albracht, S.P.J., Coremans, J.M.C.C. and Fuchs, G. (1988) Eur. J. Biochem. 171, 589-597.

Gartner, P., Weiss, D.S., Harms, U. and Thauer, R.K. (1994) Eur. J. Biochem. 226, 465-472.

Harms, U. and Thauer, R.K. (1996) Eur. J. Biochem. 241, 149-154.

6.5 Methyl-coenzyme M reductase

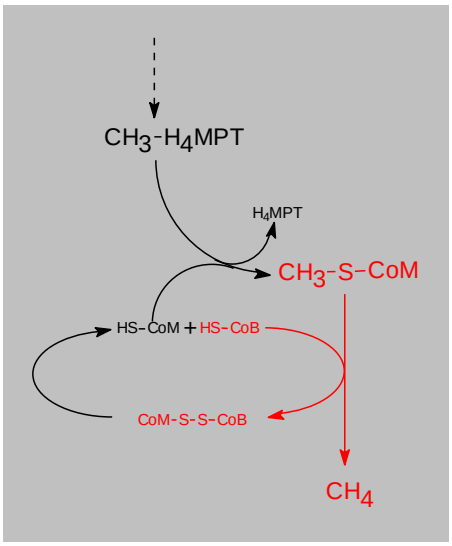

Methyl coenzyme M reductase (MCR) catalyzes the actual production of methane from methyl coenzyme M (CH_3-S-CoM). MCR contains F_{430} as prosthetic group which is a nickel porphinoid:

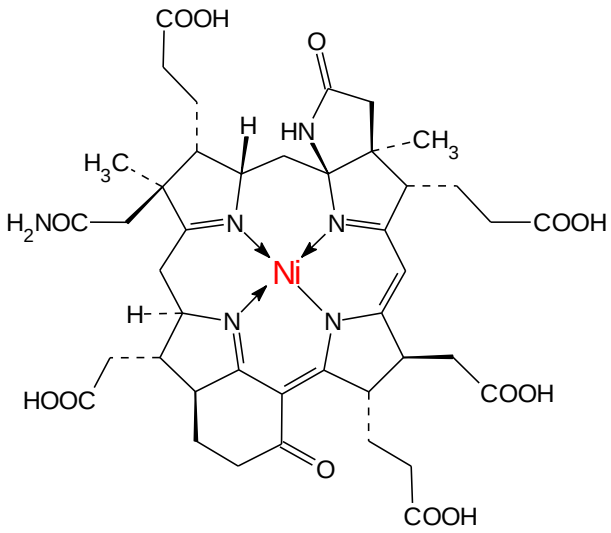

Fig. 11: Structure of F_{430}.

The four nitrogen atoms from the tetrapyrrole coordinate the nickel atom. As a result syperhyperfine structure due to the nuclear spin of the N atom (I = 1) can be detected, dependent on the orbital the free electron is in.

For the free cofactor three redox states can be obtained, 1+ (d^9), 2+ (d^8) and 3+ (d^7). Only the 1+ and 3+ states are EPR active (Fig. 12). In the 3+ state the unpaired electron is in the d_z2 orbital that points to the loosely bound axial ligands, in this example one molecule of propionitrile. This also contains a nitrogen atom, which coordinates to the nickel causing the superhyperfine structure detectable on the g_z peak. In the 1+ state the unpaired electron is in the $d_x2_{-y}2$ orbital that point towards the nitrogen ligands of F_{430}. If you look carefully you will see some hyperfine structure. The hyperfine splitting is of the same magnitude as the line width of the signal. Hyperfine structure can only be detected when the hyperfine splitting is bigger than the line width. If the hyperfine splitting is smaller it might still broaden the signal but is not be recognizable as hyperfine anymore. In that case we call it unresolved hyperfine. By looking at spectra with different EPR frequencies one will be able to determine if this is the case for a particular signal.

For MCR different signals can be found (Fig. 12). From comparison of the EPR spectra and other spectroscopical data is was concluded that the nickel in the silent state is 2+. The red1 forms show high spectroscopic similarities with those of F_{430} in the 1+ state. Therefore it is generally accepted that the nickel in the red1 form is in the 1+ state too. Note that there are two red1 forms, one with highly resolved superhyperfine structure (Red1m) and one with less resolved superhyperfine structure (Red1c). The EPR spectrum of the so-called Ox1 form is less well understood. The position of the g values cannot

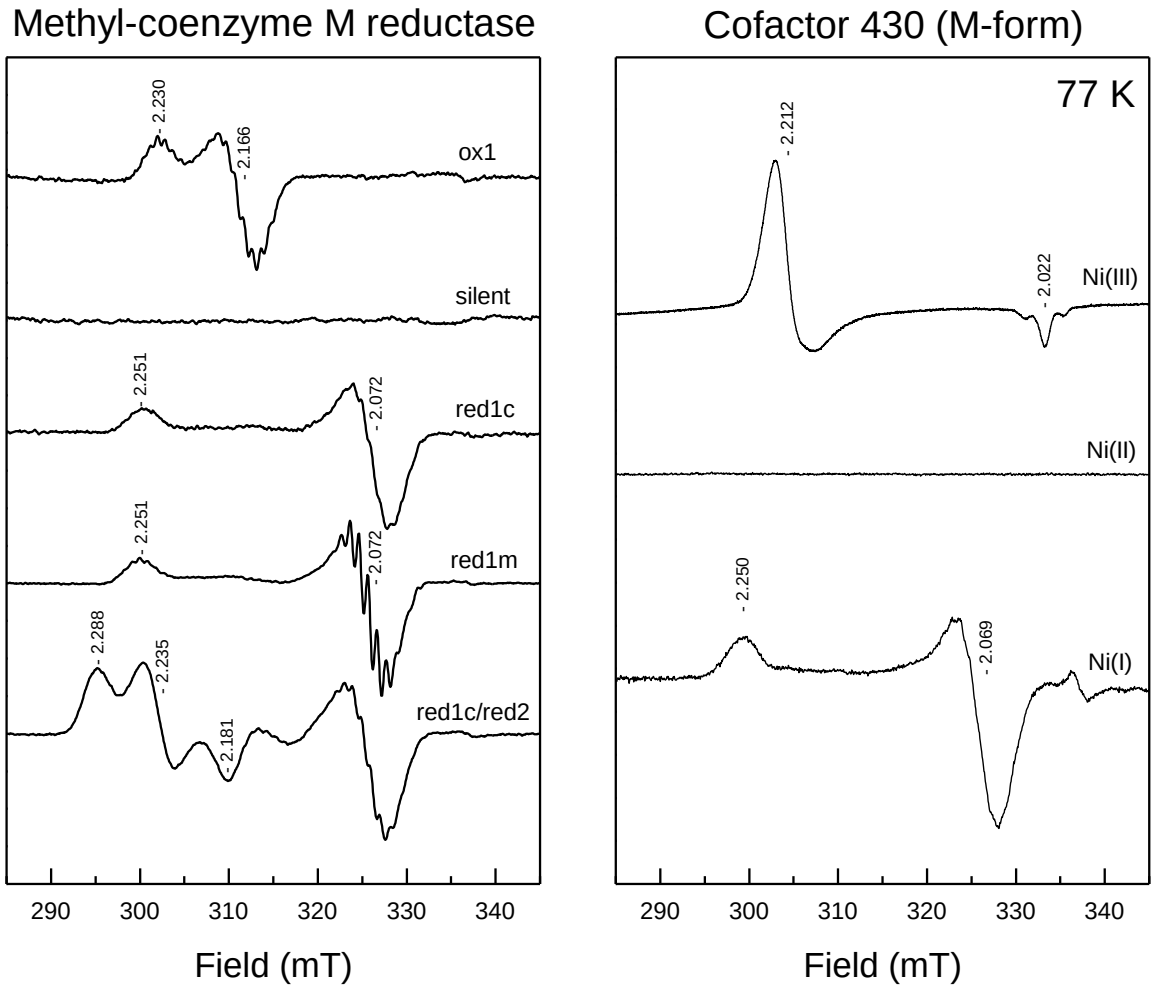

Fig. 12: EPR spectra of different forms of methyl-coenzyme M reductase from *M. marburgensis* and the free cofactor 430.

be explained based on what is known about nickel complexes. The nickel can either be 1+ or 3+. X-ray absorption data indicated that a large part of the electron density might be on a sulfur ligand bound to the nickel, which could explain the g values. With the Red2 spectrum we have the same problem. In this case it is also proposed that the rhombic EPR spectrum is due to sharing of the unpaired electron with an axial ligand bound to the nickel.

6.6 Heterodisulfide Reductase

Heterodisulfide reductase (HDR) from *M. marburgensis* is an iron-sulfur-flavin protein that catalyzes the reversible reduction of the heterodisulfide (CoM-S-S-CoB) of the thiol-coenzymes, coenzyme M (HS-CoM) and coenzyme B (HS-CoB).

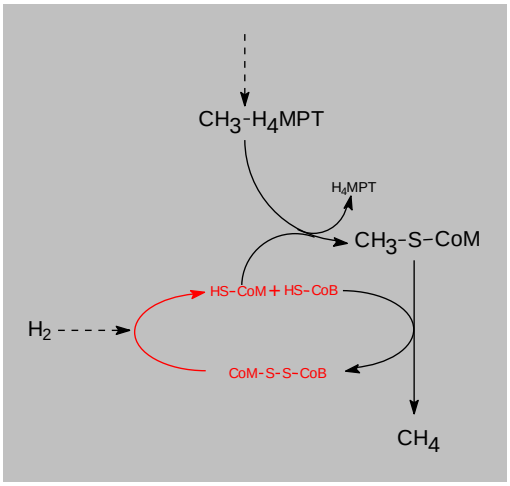

HDR is composed of three subunits, HdrA, HdrB and HdrC. HdrA contains a typical FAD binding motif and four binding motifs for $[4Fe\text{-}4S]^{1+/2+}$ clusters. HdrC contains two additional binding motifs for $[4Fe\text{-}4S]^{1+/2+}$ clusters while HdrB contains a special motif that binds a $[4Fe\text{-}4S]^{2+/3+}$ cluster that is directly involved in the catalytic reaction.

EPR spectroscopic studies indicated the presence of unique paramagnetic species that were formed upon reaction of the oxidized enzyme with HS-CoM, HS-CoB and CoM-S-S-CoB (Fig. 13). By growing cells on ^{57}Fe (I = 1/2) it was shown that the signals were iron based and probably due to iron-sulfur clusters. This can be seen in Fig. 14 where the two spectra obtained for the HS-CoM induced signal are shown. The black spectrum is the signal obtained for enzyme purified from cells grown on natural abundance iron. The red spectrum is for enzyme from cells grown on ^{57}Fe. It can clearly be detected that the ^{57}Fe signal is much broader due to unresolved hyperfine splitting due to interaction of the electron with the four iron nuclei.

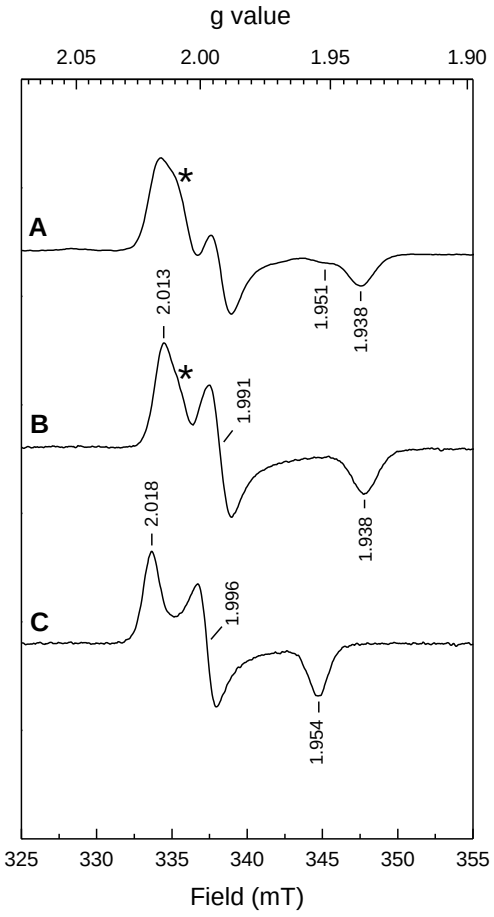

Fig. 13: EPR spectra of heterodisulfide reductase from *M. marburgensis*, (**A**) after incubation with CoM-S-S-CoB, (**B**) after incubation with HS-CoM, (**C**) after incubation with HS-CoB.

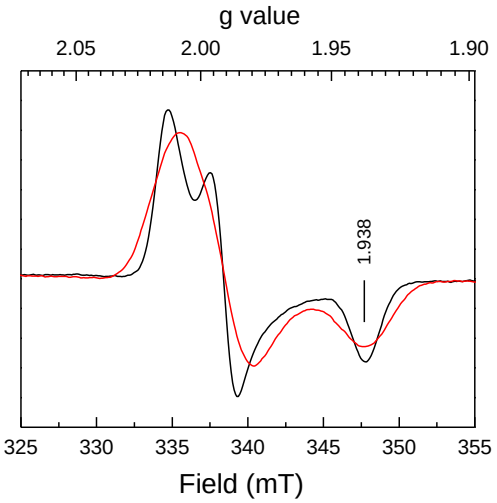

Fig. 14: EPR spectra of heterodisulfide reductase from *M. marburgensis* after incubation with HS-CoM (—) Enzyme from cells grown on natural abundance Fe. (—) Enzyme from cells grown on ^{57}Fe.

Due to the unique EPR spectra it was not clear what type of cluster was present in the active site. Magnetic circular dichroism investigations of oxidized HDR in the presence of HS-CoM or HS-CoB, however, confirmed that HDR contains a 4Fe-type cluster in its active site that is involved in disulfide reduction.

There are two models to explain the EPR signals. In the first model (Fig. 15, A) there is also an active disulfide in the active site present. The substrate, in this case HS-CoM, reacts with this disulfide and one of the disulfide sulfurs coordinates to the cluster as a way to delocalize electron density on this sulfur. In a second model (Fig. 15, B) the substrate binds directly to the cluster.

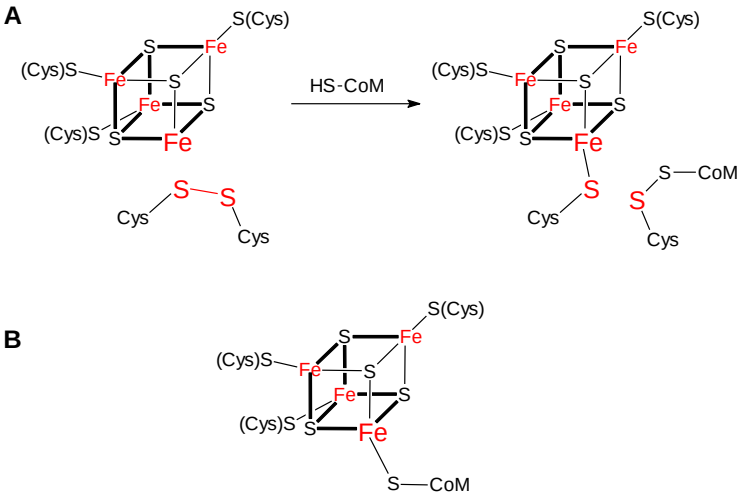

Fig. 15: Possible structures for the reaction intermediate in the active site of heterodisulfide reductase from *M. marburgensis* upon incubation with HS-CoM.

Reference:

Madadi Kahkesh, S., Duin, E.C., Heim, S., Albracht, S.P.J., Johnson, M.K., and Hedderich, R. (2001) *Eur. J. Biochem.*, 268, 2566-2577.

6.7 EPR signals in whole cells

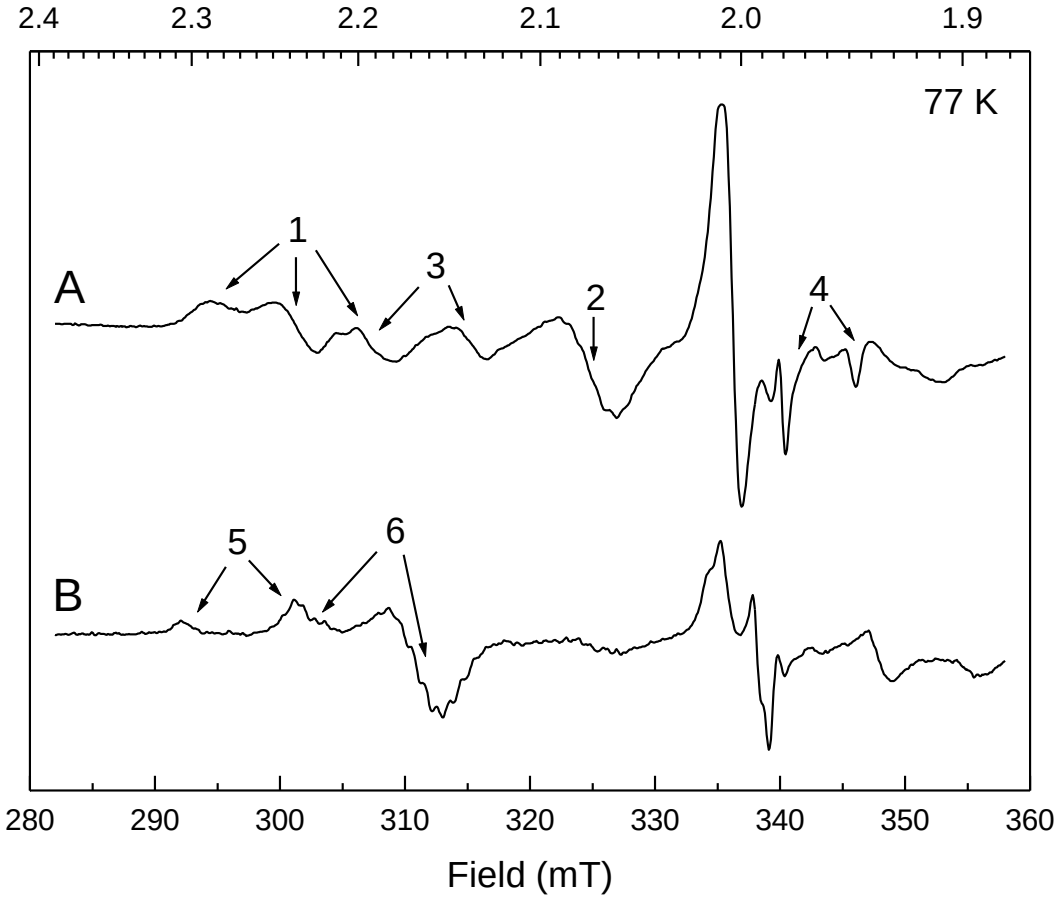

Fig. 16: EPR spectra of cells *from M. marburgensis*. (A) Cells after 30 min gassing with 100% H_2. (B) Cells after 30 min gassing with 80% N_2/20% CO_2.

Some of the enzymes in *M. marburgensis* are highly abundant. For example it has been estimated that the methyl-coenzyme M reductase enzyme constitutes about 10% of the total protein present in the cell. Therefore cells of these species and also cell extracts can be used to study the behavior of some of these proteins. Fig. 16 shows two EPR spectra of whole cells which have been gassed with 100% H_2 (Fig. 16, trace A) or with 80% N_2/20% CO_2 (Fig. 16, trace B). Can you recognize the different methanogenic metalloenzymes?

Solution:

1: Methyl-coenzyme M reductase, red2 form.
2: Methyl-coenzyme M reductase, red1c form (g_y and g_x).
3: Hydrogenase, Ni-C form (g_x and g_y).
4: Formylmethanofuran dehydrogenase (two g_z peaks).
5: Hydrogenase, Ni-A form (g_x and g_y).
6: Methyl-coenzyme M reductase, ox1 form.